Original Research Article

Ultrastructure of Glial Brain Tumors and Pathomorphological Assessment of Changes After Cryodestruction

ABSTRACT

Background: The role of cryosurgery in modern oncological practice is steadily growing. Stereotactic cryodestruction of gliomas is one of minimally invasive techniques helps to carry out more sparing surgical interventions in patients with glial tumors of deep, functionally significant structures. This study was aimed at studying the effects of cryoablation at the cellular level.

Materials and methods: The authors analyzed the results of histological examination of the surgical material of 6 patients with supratentorial glial brain tumors of various degrees of malignancy. The sampling of the material for the study was carried out immediately before the introduction and after the extraction of the cryoprobe.

Results: A comparative electron microscopic examination in the areas of glial tumors after the cryodestruction showed manifestations of its gross destruction: ruptures of nervous tissue,

fragmentation of the cytolemma and karyolemma, vacuoles of various sizes, including near the nucleus, various disorders of the chromatin structure, accumulation of gliofibrils in the absence of other organelles. The structure of myelin fibers in the glioma site after the cryotherapy was very diverse: there were myelin fibers with intense myelinopathy and axonopathy. The neuropile around the cells had a low electron density, or bundles of gliofibrils were found in it.

Conclusions: At EME of tumor tissue we found not only the specific, previously described signs of damage at the tissue level, but also ultrastructural changes. The results presented by us show that the tumor cryodestruction not only results in direct destruction of tumor cells, but also triggers other mechanisms of glioma cell death. The above points to the need for prospective randomized controlled clinical studies with a large number of patients to determine the effectiveness of this promising method for the treatment of patients with glial brain tumors.

Keywords: glioma, cryodestruction, electronic microscopy, histopathology

1. INTRODUCTION.

Cryosurgery is widely used in modern oncological practice for ablation of primary extracerebral tumors, metastatic lesions [1, 2], as well as for the destruction of brain tumors [3-5]. The histological effects of cryodestruction in gliomas have been studied only in in vitro experiments, using animal tumor models or based on MR imaging data in a clinic setting [6-8]. Histological and ultramicroscopic changes immediately after exposure of a glial tumor to low temperatures in humans were not previously investigated. The study of the effect of cold ablation at the molecular, cellular and organ levels can help expand the boundaries of its clinical application in neuro-oncology. The purpose of our study was to analyze the effects of cryoablation at the cellular level.

2. MATERIALS AND METHODS.

We have analyzed the results of histological examination of the surgical material of 6 patients with supratentorial glial brain tumors of various degrees of malignancy who had a surgery at the Neurosurgery Clinic of Military Medical Academy named after S.M. Kirov in 2020-2021, their demographic and molecular genetic characteristics are shown in the table.

Table. Patient characteristic (n=6)

№	Sex	Age, years	Hystopathology	IDH1/2 mutation	1p/19q co-deletion	Ki-67, %
1	f	19	ODG	+	+	4
2	f	38	DA	not det.	not det.	not det.
3	f	20	DA	-	-	2
4	m	34	ODG	+	+	8
5	f	32	AODG	+	+	15
6	f	29	ODG	+	+	4

Histological classification of the tumors was made according to the 2016 WHO classification [9]. Stereotactic cryodestruction of tumors was performed using a cryosurgical device with solid carbon dioxide (dry ice) with a carrier temperature of about -78°C (195°K) [10]. Dry ice was chosen as the cooling agent. Acetone was used as a coolant to transfer the low temperature into the cryoprobe cooling chamber, which made it possible to reach a temperature of -70°C in the cryotherapy center [11, 12]. The exposure time of one cold exposure cycle during the surgery was at least 6 minutes, and a repeated cryotherapy cycle was performed at each target point after defrosting. The total time of the two freeze-thaw cycles was about 20 minutes [13, 14].

Stereotactic guidance of the cryosurgical instrument to the target points was made using a domestic computerized stereotactic system [15] and the Integra CRW stereotactic system (Integra, USA). Preoperative stereotactic marking was performed using high-field MRI scanners with a magnetic field strength of 1.5 T.

During the surgery (before and after two cryodestruction cycles) a biopsy of glioma tissue for electron-microscopic examination (EME) was taken from 6 patients immediately before the introduction and after the extraction of the cryoprobe, which was then processed according to standard methods for electron microscopy [16] and poured into a mixture of resins (epon-araldite). Semi-thin slices (~1 microns thick) were made from the resulting blocks using the LKB3 ultratome and stained with toluidine blue using Nissl's method. Then the working surface of the blocks was cut off for the subsequent manufacture of ultrathin sections (~300 nm thick), which were placed on metal meshes and contrasted with Reynolds lead citrate and uranyl acetate. After contrasting, the ultrathin sections were analyzed using a JEM-100CX transmission electron microscope (Jeol, Japan).

At the EME of the glioma structure of patients all the elements of the taken nervous tissue of the brain were examined, namely: cells, nerve fibers (myelin and non-myelin), synapses, vessels and neuropile as a whole.

3. RESULTS.

Histological examination showed different variants of glial tumors in all the patients. At the light-optical level, there were no differences in the structure of tumor tissue before and after cryoablation (Fig. la, b).

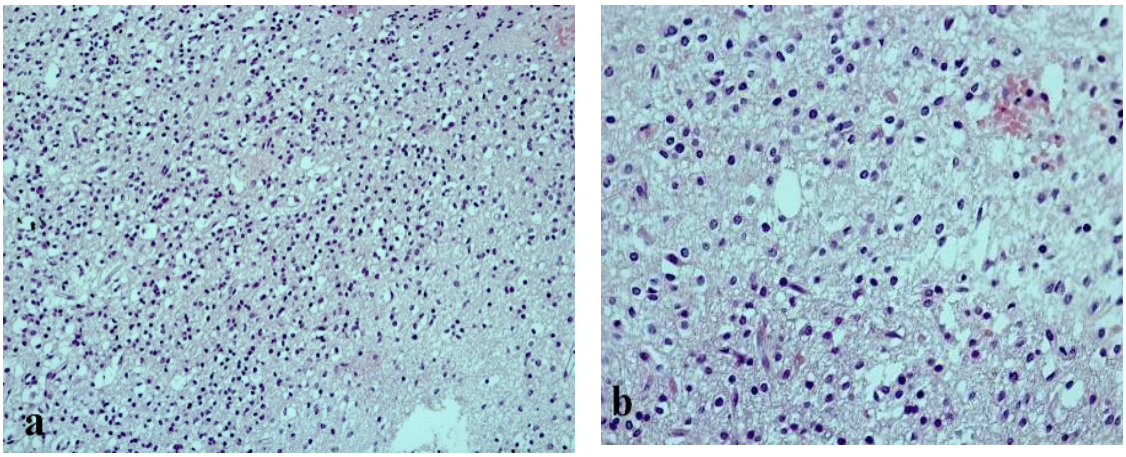

Figure 1. Oligoastrocytoma (stained with hematoxylin and eosin)

a - before cryodestruction. Magnification x200.

в - after cryodestruction. Magnification x400.

The tumor is constructed from relatively monomorphic cells with a uniform distribution in different areas. The shape of the nuclei is predominantly rounded with a light nucleoplasm. The cytoplasm of cells is optically empty, surrounded by a cell membrane. In some places the cells form "honeycomb-like" structures. There is a large number of capillaries without any signs of endothelial proliferation.

At comparative EME (before and after cryoablation) nerve tissue ruptures were observed in areas of glial tumors after cryodestruction as manifestations of its gross destruction (Fig. 2a, b).

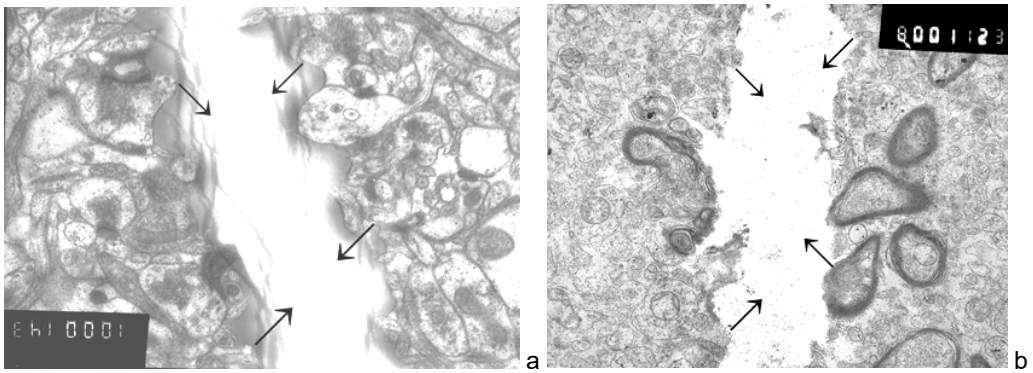

Figure 2. A trace of cryodestruction (a transparent slit in both images, arrows). Magnification: a – x10 000; b – x8000.

In the tumor cells there were "naked" nuclei with an atypical chromatin structure diffusely distributed over the karyoplasm in the form of large lumps. In these nuclei, a very large vacuole from the exfoliated portion of the karyolemma and a small detachment of the karyolemma along the entire perimeter of the nucleus were found. Fragmentation of the cytolemma and karyolemma, vacuoles of various sizes, including near the nucleus and mitochondria, were also found (Fig. 3a). At the same time, there was no karyolemma in the contact area of the vacuole and the nucleus. The accumulation of gliofibrils in the absence of other organelles can be considered important signs of changes in the cell structure (Fig. 3b). In the cytoplasm, which had no clear boundaries, there were vacuoles around the nucleus, as well as dense moderately osmophilic corpuscles, which were probably destroyed mitochondria. A cytoplasm rupture was seen near the nucleus (Fig. 3b). The neuropile around these cells was characterized by a low electron density, but bundles of gliofibrils were also found in it (Fig. 3c). The appearance of so-called "growth flasks" in tumor cells, in which a large vacuole could be located, also turned out to be interesting (Fig. 3c).

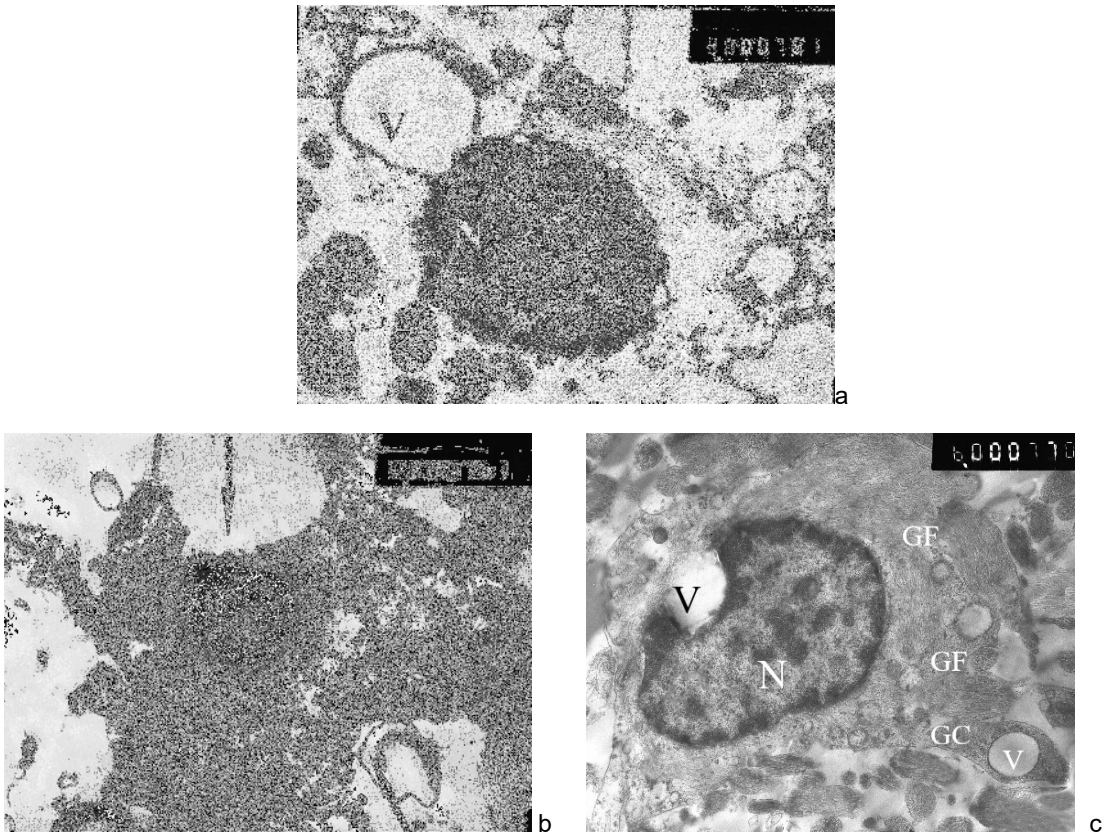

Figure 3.

a – the nucleus (N) of a tumor cell with an atypical (diffusely dense) chromatin structure and a large vacuole (V) formed by a detached section of the karyolemma. Mch – mytochondria. Magnification x8 000.

b – a tumor cell with a dense apoptotic body (AB) instead of a nucleus and destruction of the cytolemma and karyolemma (arrows). Magnification x5 000.

c – a tumor cell with large vacuoles (V) near the nucleus (N) and in the growth cone (GC). There are many gliofibrils (GF) in the cytoplasm. Magnification x8 000.

After cryodestruction of glioma tumor cells with changes in the type of necrosis were encountered. In case of necrosis, the structure of the tumor cell looks very hyperchromic, and the nucleus and cytoplasm are indistinguishable (Fig. 4a).

Among the various changes in chromatin in the nuclei of tumor cells its structure disorders were quite often noted. In some cases, chromatin in the nucleus formed dense lumps of different sizes, in others – a homogeneous hyperchromic structure. Especially interesting were the pictures of destruction of tumor cells with disorders of their karyolemma in some areas of the biopsy, as a result of which part of the chromatin was outside the nucleus. Also, in such cells, the cytoplasm was destroyed and the cytolemma was absent. The neuropile around these cells, as a rule, had a low electron density (Fig. 4b).

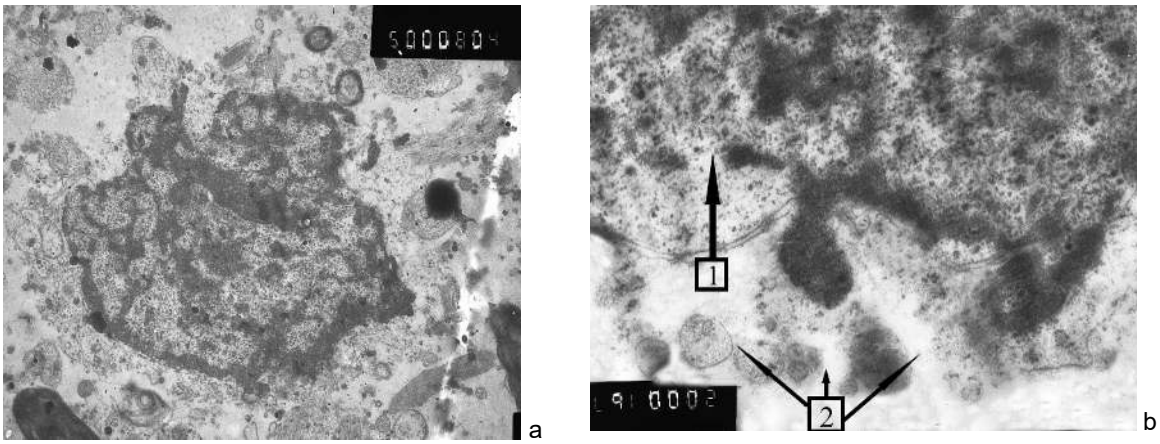

a b

Figure 4. A tumor cell in a glioma site after the cryotherapy.

a – necrosis of the tumor cell: in the right part of the image there is a site of destruction of

the neuropile in the form of a transparent slit. Magnification x8000.

b – arrows – disordered areas of the karyo- (1) and cytolemma (2).

Magnification x20 000. The details are in the text.

The structure of myelin fibers in the glioma site after the cryodestruction was very diverse. Thus, in most of the fibers, indentation of individual sections of the myelin sheath into the axial cylinder or protrusion outward was observed (Fig. 5a). At the same time, in another part of the fibers, there was more or less pronounced defibration of myelin lamellae (Fig. 5b). At the same time myelin fibers were located in a neuropile with a low electron density.

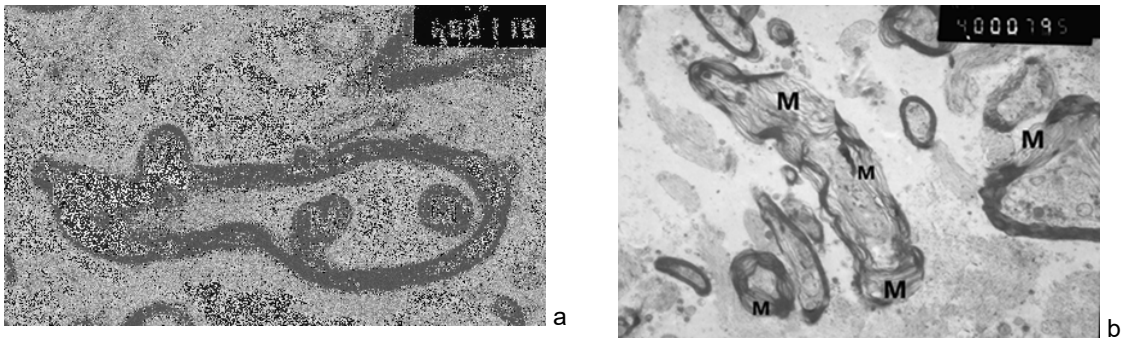

a b

Figure 5. Different condition of myelin fibers (MF).

M — myelin. Magnification: a – x6 000; b – x4000.

160

161 Free myelin fragments were found in the axial cylinders of myelin fibers, and other hyperosmiophilic
162 fragments of unclear genesis were often found in both myelin and myelin-free fibers. The shell of the
163 myelin-free fibers was partially damaged (Fig. 6).

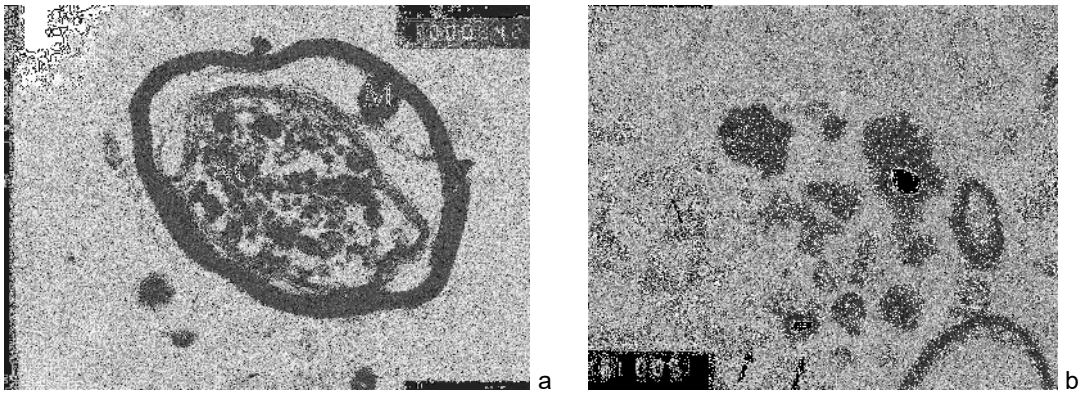

a b

Figure 6. Nerve fibers with hyperosmyophilic inclusions in the axial cylinder (AC):

a – myelin fiber, b – myelin-free fiber. M – myelin. The arrows point to the areas of rupture of the shell of the AC of the myelin-free fiber.

Magnification: a – x10 000; b – x15 000.

164

165 In addition to these disorders of myelin fibers after the cryodestruction of glioma, there was occasionally a
166 sharp thinning of the myelin sheath and high transparency (edema?) of the axial cylinder (Fig. 7a). And,
167 on the contrary, in a number of myelin fibers there was an intense swelling of the shell and almost
168 complete disappearance of the axial cylinder (the so-called hypermyelination) (Fig. 7b). In the space
169 surrounding the fibers a decrease in the electron density was noted.

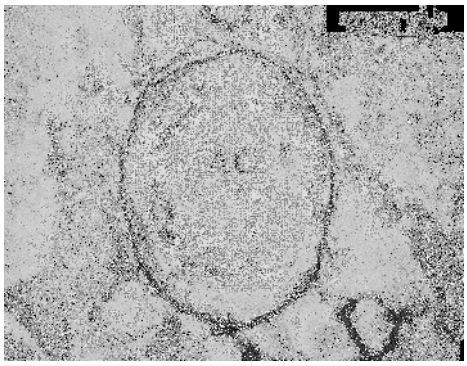
a

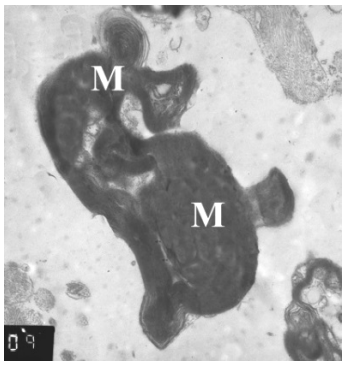

b

Figure 7. Myelin fibers with different disorders of myelin (M) and axial cylinder (AC).

Magnification: a – x4 000; b – x6 000.

170

171 Clusters of hyperosmiophilic inclusions of unclear origin and different (often large) sizes were found in the
172 neuropile among myelin fibers. Most likely, these inclusions were fragments of cells and nerve fibers
173 destroyed by cryodestruction (Fig. 8).

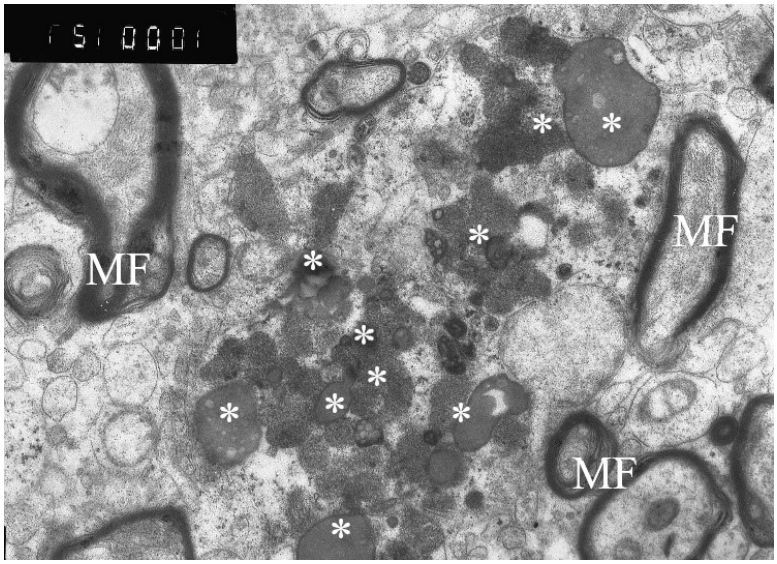

Figure 8. * - Hyperosmiophilic inclusions in the neuropile.

MF — myelin fiber. Magnification x5 000.

174

175 After the cryodestruction of glioma focal clusters of gliofibrils were often found in the almost transparent
176 neuropile (Fig. 9a). Their uncharacteristic accumulation in the cytoplasm was also observed in parts of
177 oligodendrocytes. In such cells the cytolemma was destroyed both near the gliofibrils and in other parts of
178 the cell (Fig. 9b). Myelin fibers with pronounced myelin and axonopathy were observed near these tumor
179 cells. The first was manifested by compaction or thinning of myelin lamellae, and axonopathy – by an
180 increase in the electronic transparency of the axial cylinder.

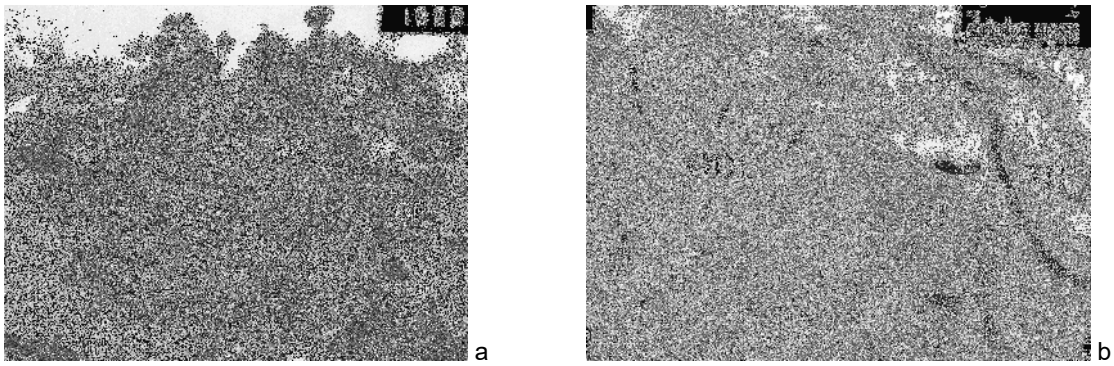

Figure 9. Focal clusters of gliofibrils (GF):

a – in the neuropile. Magnification x15 000.

b – in the cytoplasm of oligodendrocyte (ODC) and in close contact with the cell. There are areas of the ODC cytolemma destruction (arrows). GF – gliofibrils; MF – myelin fiber with signs of myelinopathy and axonopathy. Magnification x8 000

181

182 After cryodestruction of gliomas synapses with various disorders of their organization were often found in
183 areas of the neuropile with increased transparency, with myelin and myelin-free fibers. The contact areas
184 of these synapses were blurred (Fig. 10a, b). Among the synapses (as happens in a normal brain without
185 a tumor), in addition to single-pole ones (Fig. 10a), there were single bipolar ones (Fig. 10b). Synaptic
186 vesicles and mitochondria were not always found.

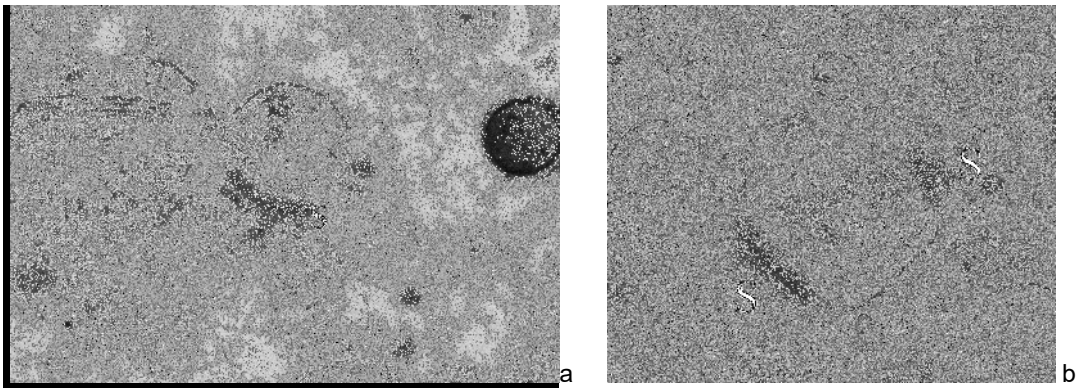

Figure 10. Different types of synapses (S) after the cryodestruction:

a – unipolar synapse. Magnification x40 000.

b – bipolar synapse. Magnification x20 000.

187

188 Before the cryodestruction of glioma, the walls of most capillaries as a whole remained intact (Fig. 11a).
189 After cryotherapy of the tumor, erythrocytes were found in the lumen of the capillaries, forming coin
190 columns (capillarostasis) in a number of vessels (Fig. 11b). Signs of destruction were detected in the
191 capillary endothelium. Part of the erythrocytes in the form of single cells or columns (as a consequence of
192 the increased permeability of the blood-brain barrier or the destruction of the wall) was located outside the
193 capillaries (Fig. 11c, d).

194

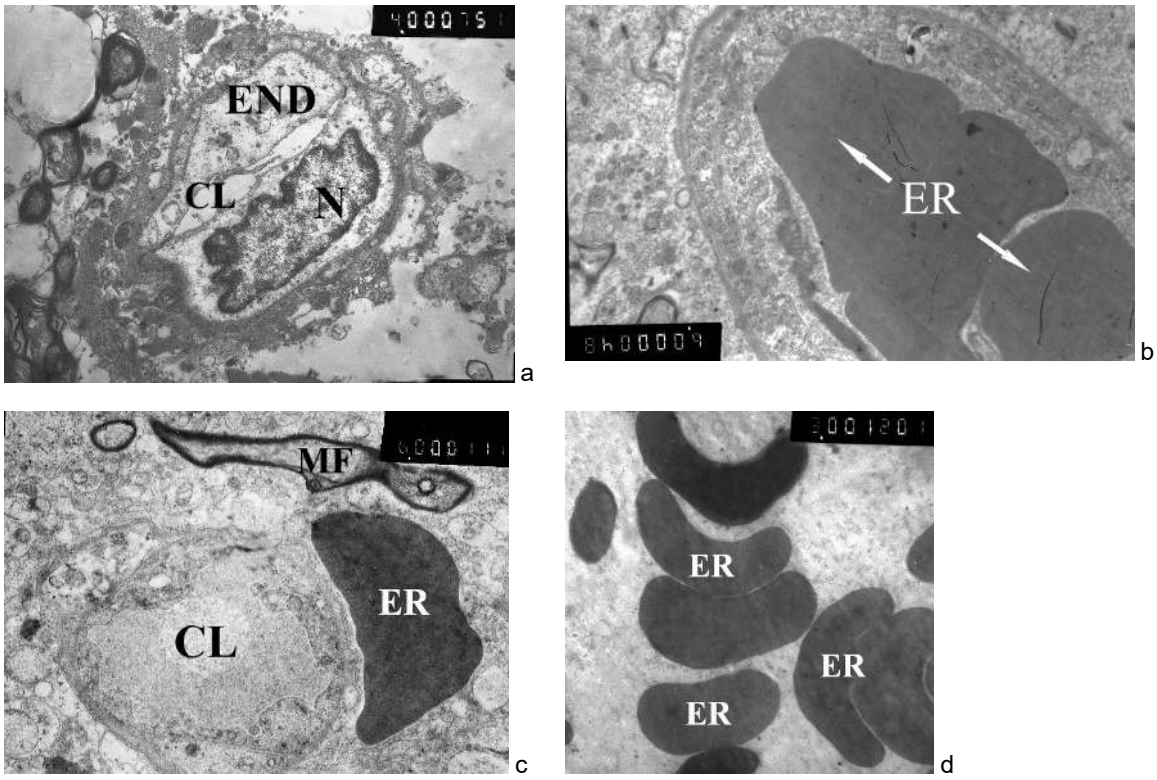

Figure 11. Erythrocytes and vessels before (a) and after the cryodestruction of glioma (b, c, d).

ER – erythrocytes, N – the nucleus of endotheliocyte, END – endotheliocyte, CL – capillary lumen, MF – myelin fiber. Magnification a – x4 000; b, c – x6 000; d – x3 000.

4. DISCUSSION.

Neurosurgical intervention is the first stage of the treatment of gliomas which continue to take a leading position in frequency of occurrence and account for 26% of all tumors of the central nervous system (6.57 per 100,000 population) [17]. The improvement of neuroimaging methods, the development of modern neuronavigation, and minimally invasive techniques help to find much less traumatic access to intracerebral neoplasm. At the same time, it becomes possible to perform more sparing surgical interventions for glial tumors of deep, functionally significant structures and thereby expand the indications for surgical treatment of patients in whom, due to the high risks of complications, neurosurgical care was previously limited only to diagnostic biopsy [5,15,18,19]. One of such methods is stereotactic cryodestruction of gliomas [20]. The purpose of our study was to analyse the effects of cryoablation at the cellular level.

There are two main known mechanisms by which cryoablation induces cell damage and death. Firstly, it is a direct destruction of cells caused by intracellular/extracellular formation of ice crystals, and secondly, it is microcirculatory insufficiency that occurs during thawing [11]. In the experimental works of a number of authors, it was found that histological examination of cryogenic lesions showed central coagulation necrosis surrounded by a relatively thin peripheral zone. Within this peripheral region apoptosis and secondary necrosis occur, which provide important mechanisms for continued cell death [21,22]. In studies of glioma C6 performed a few hours after the cryodestruction, the specimens were stained with hematoxylin and eosin and the presence of destruction of tumor cells, densification of nuclei and coagulation necrosis was shown. A week after cryoablation obvious stagnation and hemorrhage were observed with the formation of granulation tissue along the edge of the destruction site. 7 days after the cryoablation the development of apoptosis phenomena was noted mainly around the foci of cryodestruction in the form of nuclear densification, the appearance of yellowish-brown nuclei and chromatin marginalization [7,8,23]. In our practice during histological examination of tumor tissue immediately after the cryodestruction, morphological changes at the light-optical level were not found in the analyzed material. This discrepancy may be due to the difference in the time of sampling the material

for histological examination. In all the literature sources presented, the sampling of the analyzed material was carried out either in a few hours or days after the cryotherapy. While studying the material taken immediately after cryoablation we registered only ultrastructural changes. At EME of tumor tissue we found not only characteristic signs of damage at the tissue level (previously described during histological examination of tissue that underwent cryoablation *in vivo*), but also features of these changes at the cell level. According to the results of our study, cells and their nuclei were destroyed with a destruction of the karyolemma, as a result of which part of the chromatin was outside the nucleus. The cytoplasm in such cells was also destroyed, and the cytolemma was absent. The structure of myelin and myelin-free fibers also changed greatly, which was manifested both by edema of the axial cylinders and their slagging. In addition, clusters of phagolysosomes and osmiophilic inclusions were observed in the neuropile, which was a consequence of the destruction of both cells and fibers. This was also indicated by the frequent detection of clusters of gliofibrils both in the neuropile and in the cytoplasm of tumor cells. Synapses with various disorders of the synaptocomplex were observed in the neuropile with myelin and myelin-free fibers. Vascular effects were also found after the cryodestruction of glioma: free erythrocytes, columns of erythrocytes (signs of capillarostasis), often occurring singly and in groups, were observed in the microcirculatory vessels and outside, which is an indication of both cryodestruction-initiated blood flow disorders and indirect evidence of damage to the blood-brain barrier.

All this may be due to the fact (as is known from ultrastructural freezing experiments) that water crystallization occurs in the intracellular and extracellular spaces. Ice inside the cell forms at very high cooling rates and causes immediate damage to the cellular components. Extracellularly formed ice causes dehydration of surrounding cells. Due to the resulting osmotic shift, small vessels can expand twice as much as their normal diameter. It results in a destruction of the structural integrity of the microcirculatory vessels and no blood supply to those cells that were not directly damaged by cryoablation. In addition, contacts between endotheliocytes become loose and the endothelial layer of capillaries begins to leak fluid, which leads to an increase in the amount of interstitial fluid and immunocompetent cells in the parenchyma [24,25].

The mechanisms of glioma cell death in patients undergoing cryodestruction may be different due to the heterogeneous temperature distribution. Therefore, parts of the tumor adjacent to the cryoprobe may undergo direct necrosis, others die by apoptosis, and some cells on the periphery of cryotherapy may survive. However, many triggered mechanisms of cell death can effectively induce an immune response.

Experimental studies by a number of authors have shown that cryoablation induces not only the death of tumor cells, but also enhances cellular immunity and antitumor immune response x8б26ъ. In *in vitro* experiments with several human glioblastoma cell lines, another mechanism of antitumor action of the cryoablation was also found. The extract of glioma cells after cryodestruction suppressed cell proliferation and invasion, and even moderate cooling (up to 33°C) strongly suppressed both cell proliferation and migration, and deep cooling (up to 28°C) completely stopped both these processes and changed the morphology of the cell [23,27].

One of the possible mechanisms of antitumor action triggered by the cryodestruction (in addition to the direct death of tumor cells) is the formation of anti-nuclear antibodies to tumor cells. Such antibodies have a special role in regulating cell division and death [28-30], they are able to penetrate living cells and connect with the nucleus [31, 32]. Perhaps they are the cause of glioma cells death outside the foci of cryodestruction.

CONCLUSION

Thus, the results presented by us of the detailed EME of glioma, performed for the first time, showed that tumor cryodestruction not only leads to the direct destruction of tumor cells, but also triggers other mechanisms of glioma cell death. The literature experimental data and the results of previous clinical studies stated above show that it is necessary to conduct prospective randomized controlled clinical studies with a large number of patients to determine the effectiveness of this promising method for the treatment of patients with glial brain tumors.

CONSENT AND ETHICAL APPROVAL

As per university standard guideline participant consent and ethical approval has been collected and preserved by the authors.

REFERENCES

1. Prohorov GG, Belyaev AM, Prohorov DG. Fundamentals of clinical cryomedicine. Saint Petersburg – Moscow: Kniga po trebovaniyu; 2017.
ISBN 978-5-519-50992-3.
2. Gage AA, Baust JG. Cryosurgery for tumors. J Am Coll Surg. 2007;205(2):342-356.
DOI:10.1016/j.jamcollsurg.2007.03.007. PMID: 17660083.
3. Kandel EI, Peresedov VV. Stereotaxic evacuation of spontaneous intracerebral hematomas. J Neurosurg. 1985;62(2):206-213.
DOI:10.3171/jns.1985.62.2.0206. PMID: 3881565.
4. Maroon JC, Onik G, Quigley MR, Bailes JE, Wilberger JE, Kennerdell JS. Cryosurgery re-visited for the removal and destruction of brain, spinal and orbital tumours. Neurol Res. 1992;14(4):294-302.
DOI:10.1080/01616412.1992.11740073. PMID: 1360623.
5. Martynov BV, Kholyavin AI, Nizkovolos VB, Parfenov VE, Trufanov GE, Svistov DV. Stereotactic Cryodestruction of Gliomas. Prog Neurol Surg. 2018;32:27-38.
DOI:10.1159/000469677. PMID: 29990971.
6. Khalikov AD. The use of magnetic resonance imaging during stereotaxic operations on the brain and in the postoperative period. Saint Petersburg: Dissertation abstract for the degree of candidate of medical sciences, Military Medical Academy named after S. M. Kirov; 2001.
7. Li M, Zhang S, Zhou Y, Guo Y, Jiang X, Miao L. Argon-helium cryosurgery for treatment of C6 gliomas in rats and its effect on cellular immunity. Technol Cancer Res Treat. 2010;9(1):87-94.
DOI:10.1177/153303461000900110. PMID: 20082534
8. Li M, Liu J, Zhang SZ, et al. Cellular immunologic response to primary cryoablation of C6 gliomas in rats. Technol Cancer Res Treat. 2011;10(1):95-100.
doi:10.7785/tcrt.2012.500183. PMID: 21214292
9. Louis DN, Perry A, Reifenberger G, et al. The 2016 World Health Organization Classification of Tumors of the Central Nervous System: a summary. Acta Neuropathol. 2016;131(6):803-820.
DOI:10.1007/s00401-016-1545-1. PMID: 27157931.
10. Anichkov AD, Nizkovolos VB. 1998. Device for cryosurgical impact. RU. Patent 2115377, July 20.
11. Gage AA, Baust J. Mechanisms of tissue injury in cryosurgery. Cryobiology. 1998;37(3):171-186.
DOI:10.1006/cryo.1998.2115. PMID: 9787063.
12. Rui J, Tatsutani KN, Dahiya R, Rubinsky B. Effect of thermal variables on human breast cancer in cryosurgery. Breast Cancer Res Treat. 1999;53(2):185-192.
DOI:10.1023/a:1006182618414. PMID: 10326796.
13. Kandel' EI, Biezin' OA. Kriohirurgiya opuholej golovnogo mozga [Cryosurgery of brain tumors]. Voprosy neirokhirurgii. 1971;35(1):3–9. Russian.
14. Chua KJ, Chou SK, Ho JC. An analytical study on the thermal effects of cryosurgery on selective cell destruction. J Biomech. 2007;40(1):100-116.
DOI: 10.1016/j.jbiomech.2005.11.005. PMID: 16368100.
15. Polonskij JuZ, Kholyavin AI, Martynov BV et al. Stereotactic manipulator "Oreol": current state. Bulletin of the Russian Military Medical Academy. 2016;4(56):7-13.
16. Mironov AA, Komissarchik YaYu, Mironov VA. Methods of electron microscopy in biology and medicine: Methodological guide. Sankt-Petersburg: NAUKA; 1999.
ISBN 5-02-026743-0.
17. Ostrom QT, Gittleman H, Truitt G, Boscia A, Kruchko C, Barnholtz-Sloan JS. CBTRUS Statistical Report: Primary Brain and Other Central Nervous System Tumors Diagnosed in the United States in 2011-2015 [published correction appears in Neuro Oncol. 2018 Nov 17;:null]. Neuro Oncol. 2018;20(suppl_4):iv1-iv86.
DOI:10.1093/neuonc/noy131. PMID: 30445539. PMCID: PMC6129949.
18. Karampelas I, Sloan AE. Laser-Induced Interstitial Thermotherapy of Gliomas. Prog Neurol Surg. 2018;32:14-26.

DOI:10.1159/000469676. PMID: 29990970.
19. Russell SM, Kelly PJ. Incidence and clinical evolution of postoperative deficits after volumetric stereotactic resection of glial neoplasms involving the supplementary motor area. Neurosurgery. 2003;52(3):506-516.
DOI: 10.1227/01.neu.0000047670.56996.53. PMID: 12590674.
20. Martynov BV, Kholyavin AI, Parfenov VE, Nizkovolos VB, Trufanov GE, Fokin VA et al. Metod stereotaksicheskoj kriodestrukcii v lechenii bol'nyh s gliomami golovnogo mozga [Technique of stereotactic cryodestruction in management of patients with cerebral gliomas]. Zhurnal voprosy neirokhirurgii imeni N. N. Burdenko. 2011; 75(4):17–24. Russian.
21. Baust JG, Gage AA, Bjerklund Johansen TE, Baust JM. Mechanisms of cryoablation: clinical consequences on malignant tumors. Cryobiology. 2014;68(1):1-11.
DOI: 10.1016/j.cryobiol.2013.11.001. PMID: 24239684. PMCID: PMC3976170.
22. Wen J, Duan Y, Zou Y, et al. Cryoablation induces necrosis and apoptosis in lung adenocarcinoma in mice. Technol Cancer Res Treat. 2007;6(6):635-640.
DOI: 10.1177/153303460700600607. PMID: 17994794.
23. Liu T, Wang X, Yin Z, Pan J, Guo H, Zhang S. Extracts from glioma tissues following cryoablation have proapoptosis, antiproliferation, and anti-invasion effects on glioma cells. Biomed Res Int. 2014;2014:236939.
DOI:10.1155/2014/236939. PMID: 24818132. PMCID: PMC4004080.
24. Rubinsky B, Lee CY, Bastacky J, Hayes TL. The mechanism of freezing in biological tissue: the liver. Cryo-Letters. 1987;8:379–381.
25. Giampapa VC, Oh C, Aufses AH Jr. The vascular effect of cold injury. Cryobiology. 1981;18(1):49-54.
DOI:10.1016/0011-2240(81)90005-5. PMID: 7471796.
26. He XZ, Wang QF, Han S, et al. Cryo-ablation improves anti-tumor immunity through recovering tumor educated dendritic cells in tumor-draining lymph nodes. Drug Des Devel Ther. 2015;9:1449-1458. Published 2015 Mar 10.
DOI:10.2147/DDDT.S76592. PMID: 25792805. PMCID: PMC4362656.
27. Fulbert C, Gaude C, Sulpice E, Chabardès S, Ratel D. Moderate hypothermia inhibits both proliferation and migration of human glioblastoma cells. J Neurooncol. 2019;144(3):489-499.
DOI:10.1007/s11060-019-03263-3. PMID: 31482266
28. Zajchik AM, Poletaev AB, Churilov LP. "Self " recognition and interaction with "self " as a main activity of adaptive immune system. Vestnik of St. Petersburg University. 2013;1:7-16.
29. Il'chevich NV, Lisyanyj NI, Yanchij RI. Antibodies and regulation of body functions. Kiev: Naukova dumka; 1986.
30. Zaichik ASh, Churilov LP, Utekhin VJ. Autoimmune regulation of genetically determined cell functions in health and disease. Pathophysiology. 2008;15(3):191-207.
DOI: 10.1016/j.pathophys.2008.07.002. PMID: 18760573.
31. Alarcón-Segovia D, Ruíz-Argüelles A, Fishbein E. Antibody penetration into living cells. I. Intranuclear immunoglobulin in peripheral blood mononuclear cells in mixed connective tissue disease and systemic lupus erythematosus. Clin Exp Immunol. 1979;35(3):364-375.
PMID: 378481. PMCID: PMC1537612.
32. Alarcon-Segovia D, Llorente L, Ruiz-Arguelles A. Antibody penetration into living cells. III. Effect of antiribonucleoprotein IgG on the cell cycle of human peripheral blood mononuclear cells. Clin Immunol Immunopathol. 1982;23(1):22-33.
DOI: 10.1016/0090-1229(82)90067-8. PMID: 6980072.

ABBREVIATIONS

Abbreviations in the article (in the text and in the figures): AB — apoptotic body; AC — axial cylinder; AODG — anaplastic oligodendroglioma; CL — capillary lumen; DA — diffuse astrocytoma; EME — electron microscopic examination; END — endotheliocyte; ER — erythrocyte; GC — growth cone; GF — gliofibrils; M — myelin; Mch — mitochondria; MF — myelin fiber; N — nucleus; not det. — not determined; ODC — oligodendrocyte; ODG — oligodendroglioma; S — synapse; V — vacuole.